Original Article

Horsetail Assisted Green Synthesis of Fe_3O_4@SiO_2-Pd: A Reusable and Highly Efficient Magnetically Separable Catalyst for Suzuki Coupling Reactions

Rosa Khazaei[a,*] | Ardeshir Khazaei[a] | Mahmoud Nasrollahzadeh [b,c,*]

[a]*Faculty of Chemistry, Bu-Ali Sina University, Hamedan 6517838683, Iran*
[b]*Center of Environmental Researches, University of Qom, Qom, Iran*
[c]*Department of Chemistry, Faculty of science, University of Qom, P. O. Box 37185-359, Qom, Iran*

Use your device to scan and read the article online

Citation R. Khazaei, A. Khazaei, M. Nasrollahzadeh. **Horsetail Assisted Green Synthesis of Fe_3O_4@SiO_2-Pd: A Reusable and Highly Efficient Magnetically Separable Catalyst for Suzuki Coupling Reactions.** *J. Appl. Organomet. Chem.*, **2023**, *3*(2), 123-133.

https://doi.org/10.22034/JAOC.2023.397315.1079

Article info:
Received: 14 May 2023
Accepted: 10 June 2023
Available Online: 13 June 2023
ID: JAOC-2305-1079
Checked for Plagiarism: Yes

Keywords:
Suzuki coupling reaction, Green synthesis, Fe_3O_4@SiO_2-Pd nanocatalyst, Horsetail

ABSTRACT

Fe_3O_4@SiO_2-Pd nanocatalyst was successfully synthesized from Horsetail plant (*Equisetum arvense*) that provides biosilica. The synthesized Fe_3O_4@SiO_2-Pd nanocatalyst was characterized by Fourier transform infrared, XRD, SEM, EDAX, and VSM measurements. In the Suzuki coupling process, the Fe_3O_4@SiO_2-Pd nanocatalyst's effectiveness as a catalyst was also examined. The products were characterized by NMR. The main advantage of this method is small reaction time, high percentage yield, use of natural materials, low catalyst loading, simple experimental procedure, easy work, and cleaner. This catalyst was highly recyclable and was recovered in a facile manner by employing an external magnet and reusing it several times.

Introduction

Suzuki coupling reaction between aryl halides and organoboronic acids plays a a vital part in the synthesis of nonsymmetric and symmetric biaryls [1-5], which is widely utilized in many fields, including medicine and cosmetics, pharmacology and polymers, advanced materials, and ligands [6-11]. There are several methods for the synthesis of biaryl compounds in Suzuki reactions using different catalysts [12-15]. Certain heterogeneous catalysts have lower reactivity than homogeneous ones as a result of palladium leaching [16-18]. Homogeneous catalysts suffered from drawbacks such as high operational costs, short life time, tedious work-ups, and the difficulty of separating. Therefore, it is important to design a better heterogeneous catalyst to transform aryl halides into the corresponding biaryls.

In recent years, different supporting materials have been utilized to load MNPs for Suzuki reactions, due to its low cost, thermal, and

***Corresponding Authors: Rosa Khazaei** (Miss.khazaei@gmail.com) **& Mahmoud Nasrollahzadeh** (mahmoudnasr81@gmail.com)

chemical satiability and easily removal from the reaction mixture [14-15]. But, it is crucial that these active places are accessible.

Among various supports, magnetic nanoparticles have attracted much attention due to their magnetic properties, high stability, and high catalytic activity, as well as inexpensive and simple recovery with an external magnet that can be used for the heterogeneous catalysts [19-25]. Our continuous interest in the development of environmentally sustainable methods for preparing heterogeneous catalysts [22-25], has led us to focus our investigations on the use of Horsetail as the source of biosilica (**Scheme 1**) for stabilization of palladium magnetic nanoparticles and preparation of nano-Fe_3O_4@SiO_2-Pd (**Scheme 2**) in Suzuki coupling reaction. Horsetail (*Equisetum arvense*) is a herbaceous perennial plant which can be used in medicinal chemistry due to its high silica content [26-27].

Experimental

Instruments and reagents

Chemical reagents

Chemical reagents were purchased from the Aldrich and Merck chemical companies.^{1}H-NMR spectra were recorded on a Bruker Avance DRX-400 spectrometer at 400. FT-IR spectra were recorded on a Nicolet 370 Fourier transform infrared spectrometer (Thermo Nicolet, USA) using pressed KBr pellets. UV-Visible spectral analysis was recorded on a double-beam spectrophotometer (Hitachi, U-2900). XRD measurements were carried out using a Philips powder diffractometer type PW 1373 goniometer (Cu Kα = 1.5406 A˚). The scanning rate was 2˚/min in the 2θ range from 10 to 90˚. Scanning electron microscopy was performed on a Cam scan MV2300. EDS (S3700N). Vibrating sample magnetometer was performed using a SQUID magnetometer at 298 K (Quantum Design MPMS XL).

Scheme 1. The SiO_2 synthesis from Horsetail

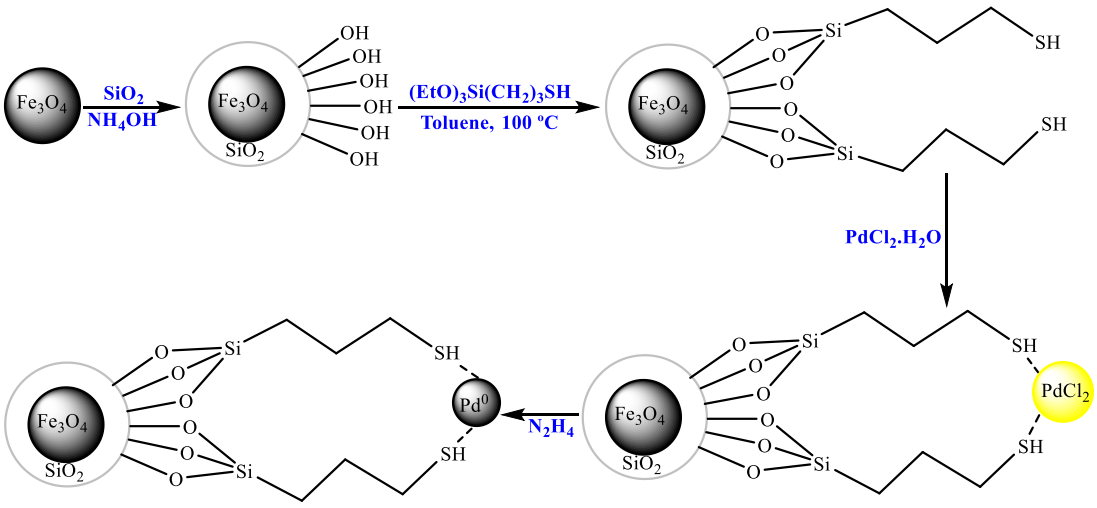

Scheme 2. The synthesis of Fe_3O_4@SiO_2-Pd nanoparticles for Suzuki coupling reactions

Preparation of Fe_3O_4 magnetic nanoparticles

Fe_3O_4 magnetic nanoparticles were synthesized according to the literature [28-31] using simple chemical coprecipitation. 4.6 g of $FeCl_2.4H_2O$ and 11.3 g of $FeCl_3.6H_2O$ were dissolved in 250 mL of deionized water into a 500 mL round-bottom flask and at 80 °C stirred until the solution was clear, and then water solution of ammonia (30 mL, 25%) was added and stirred for 2 h. At the end, black product was separated by magnetic decantation, washed with deionized water for 2 times, and then dried until 60 °C in vacuum.

Preparation of biosilica from Horsetail

Firstly, the Horsetail Plant was cleaned with distilled water many times before being dried. at 100 °C for 24 h. The reaction was performed in reflux condenser. The Horsetail (5.0 g) was added and acid-leached with HCl 10% and sulfuric acid 30 wt.% solution under stirring at 100 °C for 3 h. At the end of the reaction, brown product was filtered and washed 3 times with deionized water and dried for 5 h at 80 °C. Finally, the product was calcinated for 3 h at 700 °C to get Silicon dioxide.

Preparation of nanostructured silica-coated magnetic

The mixture of Fe_3O_4 (1.0 g), ethanol (80 mL), deionized water (40 mL) and NH_3 25% (4.0 mL) was sonicated for 30 min, and then SiO_2 (1.0 g) was combined after the addition and was refluxed for half a day. At the end of the reaction, the resulting products were washed with DI Wate three times and dried at 65 °C in vacuum.

Preparation of functionalized SiO2 magnetic nanoparticles with 3(triethoxysilyl)propane-1-thiol

This compound was prepared by refluxing for 12 h of SiO_2 magnetic nanoparticles (1.0 g) and with 3-(triethoxysilyl) propane-1-thiol (2.0 mmol) in ethanol (5.0 mL). Following the reaction time, the product was separated by centrifugation, washed with DI Wate, and ethanol and dried at 70 °C for 5 h.

Preparation of pd magnetic nanoparticles

$PdCl_2$ (100 mL, 1 mM) and earlier stage product (1.0 g) were refluxed in 10 mL of deionized water for 3 hours. The product was separated and washed with DI Wate, and then the resultant precipitate was re-dispersed in DI Wate and 0.4 mL of newly prepared N_2H_4 aqueous solution (0.25 M) was added and mixture was stirred for 2 hours. Likewise, the solution color changed into black indicating reduction of Pd^{II} to Pd(0). Finally, the black precipitate was washed with DI Wate and dried at 65 °C for 6 hours.

General procedure for synthesis of biaryls via Suzuki coupling reactions

10 mg of the nano-Fe_3O_4@SiO_2-Pd was placed in a 25 mL Schlenk tube, and then 1.0 mmol of the aryl halide in 4 mL of water/ethanol (1:1), 1.1 mmol of phenylboronic acid, 2.0 mmol of K_2CO_3 was added to reaction mixture and stirred at 90 °C. After finishing the reaction (checked by TLC), 5 mL ethanol was added and the catalyst was removed by external magnet. After removal of solvent, the remainder was purified by column chromatography. The product structure was confirmed by NMR spectroscopy.

Results and Discussion

Herein, the preparation been describe preparation of the Fe_3O_4@SiO_2-Pd nanocatalyst has been described using Horsetail (*Equisetum arvense*). The formation of Fe_3O_4@SiO_2-Pd nanocatalyst was confirmed by XRD, EDS, SEM, FT-IR, and VSM analysis.

In a typical synthesis of the Fe_3O_4@SiO_2-Pd nanocatalyst, the Pd nanoparticles (NPs) were synthesized using N_2H_4 as a reducing factor for the conversion of the Pd(II) to Pd(0) and using UV-Vis spectroscopy, the Pd NPs' production was managed. **Figure 1** displays the UV-Vis spectra of the Pd(II) and Pd NPs. The Pd(II) solution's yellow hue shifted to a dark brown hue, signifying the Pd NPs production.

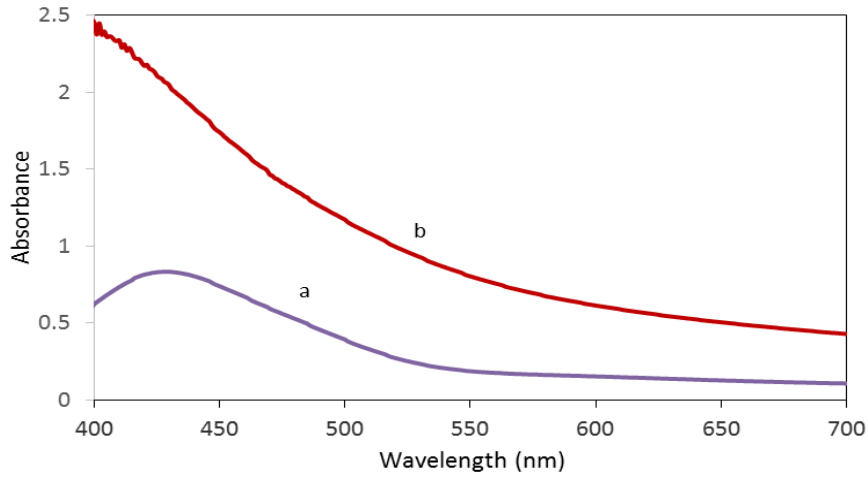

Figure 1. The UV-Vis spectra of Pd(II) (a) and Pd(0) (b)

The FT-IR spectra of the SiO_2, Fe_3O_4 and Fe_3O_4@SiO_2-Pd are illustrated in **Figure 2a-c**. As indicated in **Figure 2a**, it can be found that the peak attributed to Si-O stretching vibration put at 1000-1150 cm^{-1}. The signal of 3400 cm^{-1} was assigned to stretching of the adsorbed water molecules. The spectrum exhibits absorption band at 1500-1600 cm^{-1} for H-O-H bending vibration in water. **Figure 2b** shows the FT-IR spectrum of Fe_3O_4 the peaks at 1500-1600 cm^{-1} and 3400 cm^{-1} are related to the Fe-OH and O-H stretching modes of FeOH or adsorbed water. **Figure 2c** demonstrates the FT-IR spectrum of Fe_3O_4@SiO_2-Pd and the presence of absorbance at 1000-1150, 1500-1600, and 3400 cm^{-1} is attributed to Si-O (stretching), H-O-H (bending), and O-H (stretching).

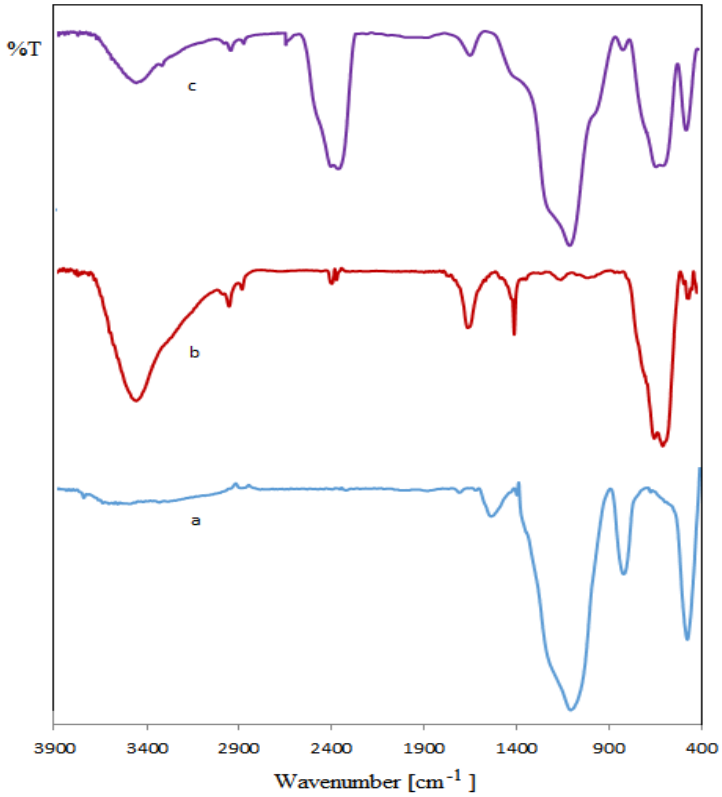

Figure 2. FT-IR spectra of the SiO_2 (a), Fe_3O_4 (b) and Fe_3O_4@SiO_2-Pd (c)

The XRD of the SiO_2, Fe_3O_4 and Fe_3O_4@SiO_2-Pd are demonstrated in **Figure 3a-c**, respectively. The peak 2θ = 21° is the characteristic peak of SiO_2 (**Figure 3a**). The diffraction peaks at 2θ value of 29. 7◦, 35.0◦, 42.7◦, 53.0◦, 56.5◦, and 62.1◦ (**Figure 3b**) corresponding, respectively, to (220), (311), (400), (422), (511), and (440) planes of the cubic Fe_3O_4 (JCPDS 19-0629). From the XRD pattern of the Fe_3O_4@SiO_2-Pd (**Figure 3c**), any typical peak for Pd nanoparticles is detected, indicating that the Pd NPs are very dispersed on the surface.

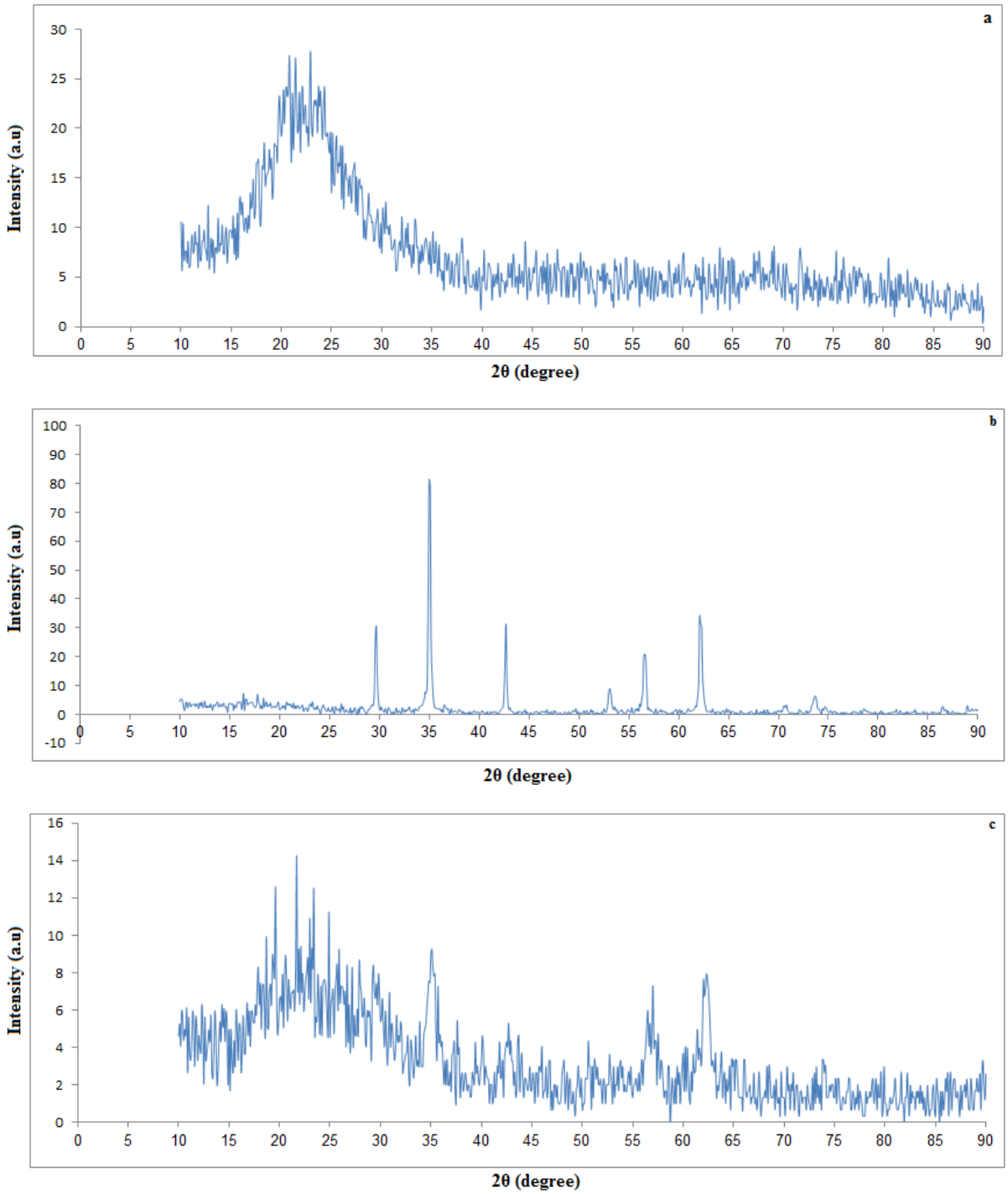

Figure 3. XRD patterns of SiO_2 (a), Fe_3O_4 (b), and Fe_3O_4@SiO_2-Pd (c)

Figure 4 and **Figure 5** illustrate SEM images and the morphology of Fe_3O_4 and Fe_3O_4@SiO_2-Pd, spherical shapes and dimensions of the particles.

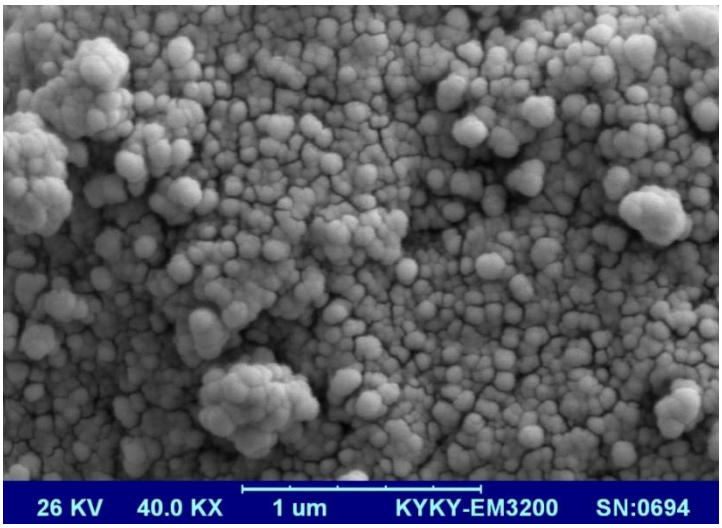

Figure 4. SEM images of the Fe_3O_4

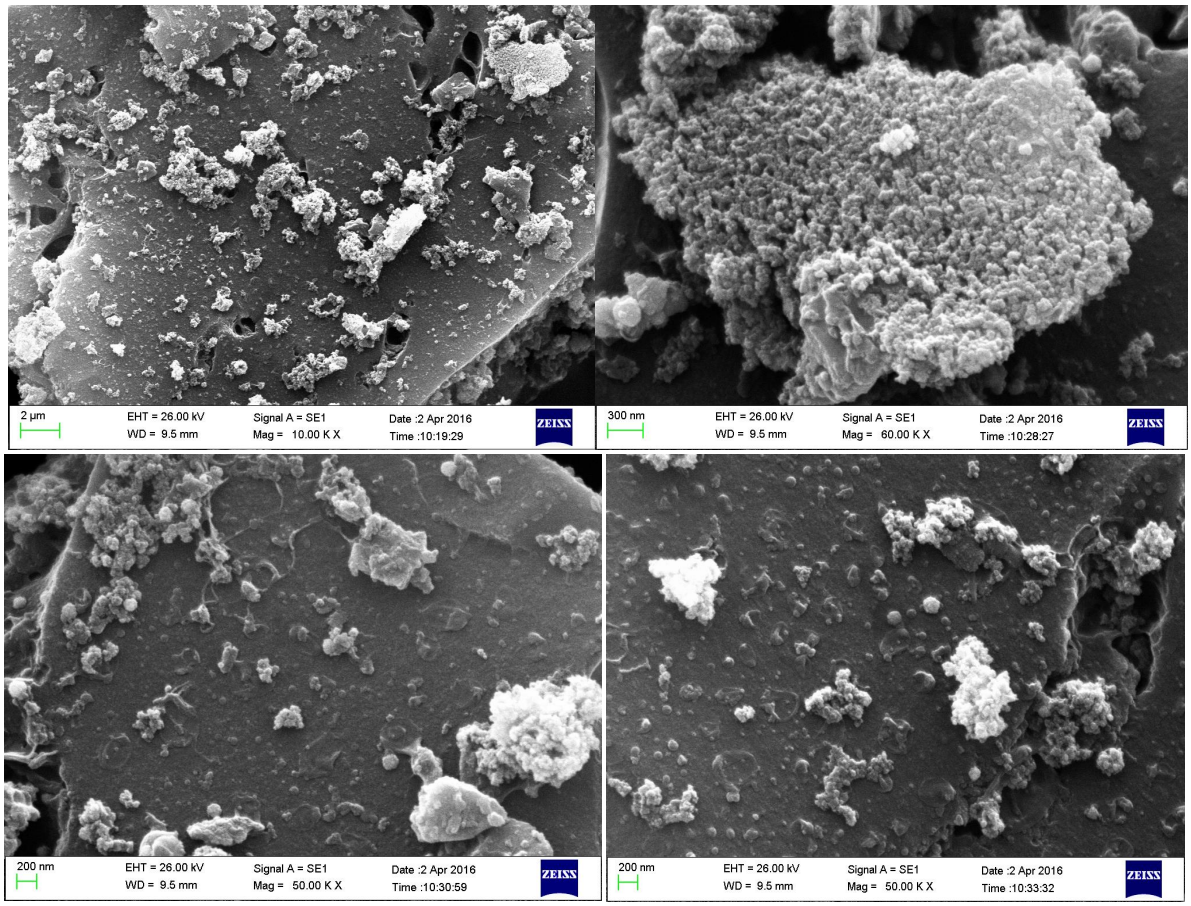

Figure 5. SEM images of the Fe_3O_4@SiO_2-Pd

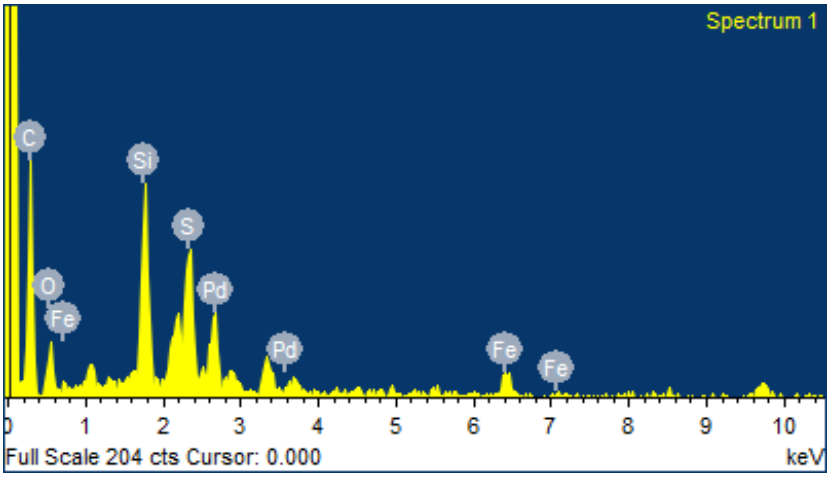

Figure 6. The EDS of the Fe_3O_4@SiO_2-Pd

Figure 6 depicts the EDS spectrum of the synthesized Fe_3O_4@SiO_2-Pd. EDS analysis reveals a strong signal for the Pd element and confirmed the formation of Fe_3O_4@SiO_2-Pd nanocatalyst.

To study the magnetic characteristic of the Fe_3O_4 and Fe_3O_4@SiO_2-Pd, the loops of particles were registered in **Figure 7** with the field sweeping from -10000 to +10000 Oe. The hysteresis loop of the Fe_3O_4 showed the highest saturation magnetization (Ms) of 60 emug^1 which is higher than the saturation magnetization of the Fe_3O_4@SiO_2-Pd. The reason of the difference is that low mass fractions of Fe_3O_4 nanoparticles were produced as a result of the thick organic matter's diamagnetic contribution. Therefore, a smaller magnetization value for the Fe_3O_4@SiO_2-Pd nanocatalyst compared to the Fe_3O_4 nanoparticles is reasonable. The Fe_3O_4@SiO_2-Pd nanocatalyst can be efficiently reused by magnet.

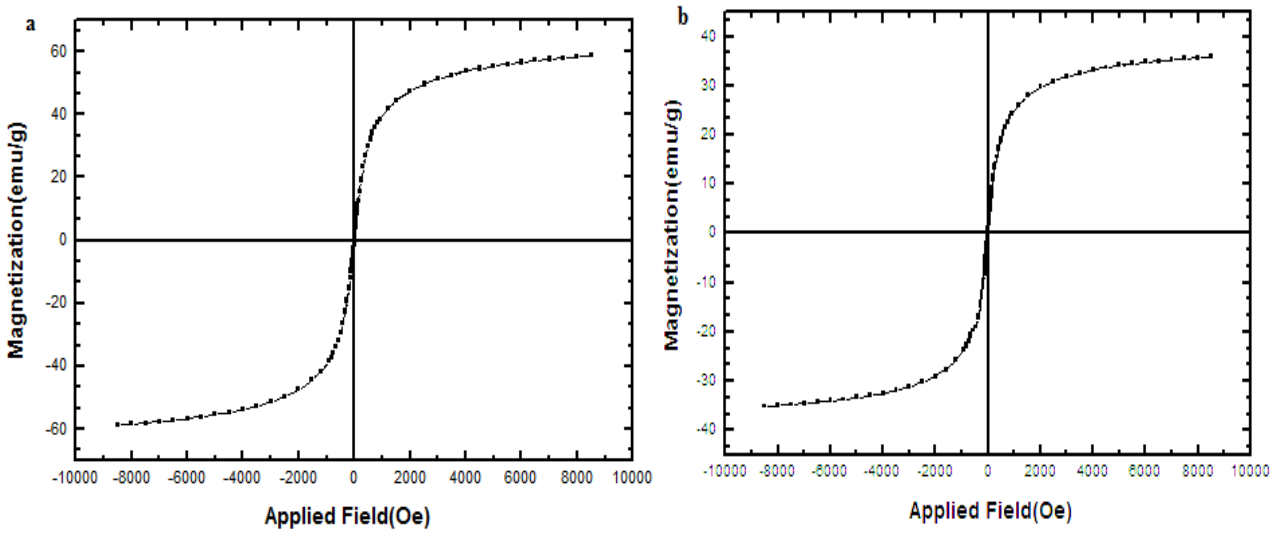

Figure 7. The vibrating sample magnetometer (VSM) analysis of the Fe_3O_4 (a) and Fe_3O_4@SiO_2-Pd (b)

Table 1. Effect of amount of catalyst, solvent and base on the Suzuki reaction of 4-bromotoluene with phenylboronic acid[a]

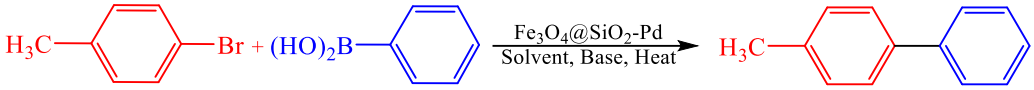

Entry	Solvent	Pd (mg)	Base	Time (min)	Yield (%)[b]
1	DMF	10	K_2CO_3	120	80
2	toluene	10	K_2CO_3	120	60
3	EtOH	10	K_2CO_3	100	70
4	H_2O	10	K_2CO_3	180	50
5	**EtOH/H_2O[c]**	**10**	**K_2CO_3**	**90**	**96**
6	EtOH/H_2O[c]	10	NaOAc	90	65
7	EtOH/H_2O[c]	10	Et_3N	90	70
8	EtOH/H_2O[c]	5	K_2CO_3	90	75
9	EtOH/H_2O[c]	20	K_2CO_3	90	96
10	EtOH/H_2O[c]	10	-	180	Trace

[a]Reaction conditions: 4-methyl-bromobenzene (1 mmol), $PhB(OH)_2$ (1.1 mmol), $Fe_3O_4@SiO_2$-Pd (mg), solvent (4.0 mL), and base (2.0 mmol) at 90 °C.
[b]Isolated yield.
[c]EtOH/H_2O= 1:1.

The $Fe_3O_4@SiO_2$-Pd was used for the Suzuki coupling reaction of phenyl boronic acids with different aryl halides. A preliminary screening proved that $Fe_3O_4@SiO_2$-Pd nanocatalyst is effective in promoting the reaction of phenylboronic acid with 4-bromotoluene. No desired product was gained in the absence of catalyst. Several solvents and base were examined. The reaction was also performed in the presence of different amount of catalyst and the results are presented in **Table 1**. It was observed that with a rise in catalyst from 5.0 to 10.0 mg, product yield is increased. It was found that a combination of $Fe_3O_4@SiO_2$-Pd (10 mg) and K_2CO_3 (2.0 equiv.) in the presence of *4-bromotoluene* (1.0 equiv) and phenylboronic acid (1.1 equiv) in EtOH/H_2O (1:1) was optimum for an efficient reaction at 90 °C (**Table 1**, entry 5).

Furthermore, the scope of the $Fe_3O_4@SiO_2$-Pd nanocatalyst was studied with various aryl halides (**Table 2**). Under these reaction conditions, aryl halides with EWG and EDG substituents completely reacted with phenylboronic acid in the Suzuki reaction in the presence of K_2CO_3 as base in H_2O/EtOH mixture and the $Fe_3O_4@SiO_2$-Pd as catalyst, affording the related biaryls in good to high yield. We recorded aryl halides containing electron donating groups on the ring giving higher yields than electron withdrawing groups. It can be seen from **Table 2**, the $Fe_3O_4@SiO_2$-Pd nanocatalyst can be employed efficiently for different aryl halides coupling reactions. According to the obtained results, substrates containing aryl iodides giving better yields than aryl bromides and chlorides. All of the biaryl compounds were characterized using ^{1}H-NMR techniques.

The distinct advantage of $Fe_3O_4@SiO_2$-Pd nanocatalyst is its recyclability and reusability. The heterogeneous nature of catalysis is an important feature from a cost viewpoint. For this purpose, Suzuki reaction of phenyl boronic acid with bromobenzene was done under optimized conditions (**Table 3**). After performing the catalytic reaction, the $Fe_3O_4@SiO_2$-Pd catalyst was separated by an external magnetic, washed with ethanol to remove all the organic substances, dried, and then reused for another run and found not to lose efficiency even after 4 runs (**Table 3**).

Table 2. Effect of Fe_3O_4@SiO_2-Pd nanocatalyst on the Suzuki coupling reaction[a]

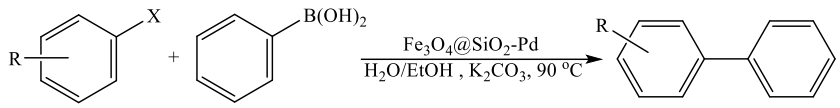

Entry	R	X	Time (h)	Yield (%)[b]
1	H	I	0.5	98
2	4-CH_3	I	1	96
3	4-$COCH_3$	I	1	96
4	2-CH_3O	I	2	90
5	4-CH_3O	I	1.5	92
6	3-NO_2	I	2	80
7	H	Br	1.5	96
8	4-$COCH_3$	Br	5	85
9	4-CH_3O	Br	4	90
10	4-CH_3	Br	4	85
11	4-Cl	Br	6	80
12	3-NO_2	Br	12	75
13	H	Cl	24	70
14	4-CH_3	Cl	24	60

[a]Reaction conditions: Aryl halide (1 mmol), $PhB(OH)_2$ (1.1 mmol), Fe_3O_4@SiO_2-Pd (mg), EtOH/H_2O (1:1, 4.0 mL), and K_2CO_3 (2.0 mmol) at 90 °C.
[b]Isolated yield

Table 3. Recyclability of Fe_3O_4@SiO_2-Pd

Entry	Fresh	Run 1	Run 2	Run 3	Run 4
Yield (%)	96	96	90	85	70

Conclusion

In summary, the Fe_3O_4@SiO_2-Pd nanocatalyst has been successfully prepared via an efficient, simple, low cost, and fast approach. EDS, XRD, SEM, FT-IR, and VSM techniques proved the formation of Fe_3O_4@SiO_2-Pd nanocatalyst. Furthermore, the Fe_3O_4@SiO_2-Pd nanocatalyst showed an efficient activity for the Suzuki reaction. In addition, the Fe_3O_4@SiO_2-Pd nanocatalyst could be removed without losing the activity by an external magnet that was reused numerous times.

Orcids

Ardeshir Khazaei
https://orcid.org/0000-0001-7990-2266

Mahmoud Nasrollahzadeh
https://orcid.org/0000-0002-4539-3544

Acknowledgements

The authors would like to gratefully thank the Iranian Nano Council and Bu-Ali Sina University for the support of this work.

References

[1]. F. Diederich, P.J. Stang, Acetylene chemistry: chemistry, biology and material science, **2006**, Wiley-VCH: Weinheim. [Crossref], [Google Scholar], [Publisher]

[2]. Z.Z. Zhou, F.S. Liu, D.S. Shen, C. Tan, L.Y. Luo, *Inorg. Chem. Commun.*, **2011**, *14*, 659-662. [Crossref], [Google Scholar], [Publisher]

[3]. F. Alonso, I.P. Beletskaya, M. Yus, *Tetrahedron*, **2005**, *61*, 11771-11835. [Crossref], [Google Scholar], [Publisher]

[4]. J.H. Kirchhoff, M.R. Netherton, I.D. Hills, G.C. Fu, *J. Am. Chem. Soc.*, **2002**, *124*, 13662-13663. [Crossref], [Google Scholar], [Publisher]

[5]. S.D. Dreher, S.E. Lim, D.L. Sandrock, G.A. Molander, *J. Org. Chem.*, **2009**, *74*, 3626-3631. [Crossref], [Google Scholar], [Publisher]

[6]. A. Markham, K.L. Goa, *Drugs*, **1997**, *54*, 299-311. [Crossref], [Google Scholar], [Publisher]

[7]. R. Capdeville, E. Buchdunger, J. Zimmermann, A. Matter, *Nat. Rev. Drug Discov.*, **2002**, *1*, 493-502. [Crossref], [Google Scholar], [Publisher]

[8]. H. Tomori, J.M. Fox, S.L. Buchwald, *J. Org. Chem.*, **2000**, *65*, 5334-5341. [Crossref], [Google Scholar], [Publisher]

[9]. M. Kertesz, C.H. Choi, S. Yang, *Chem. Rev.*, **2005**, *105*, 3448. [Crossref], [Google Scholar], [Publisher]

[10]. S. Lightowler, M. Hird, *Chem. Mater.*, **2005**, *17*, 5538-5549. [Crossref], [Google Scholar], [Publisher]

[11]. X. Zhan, S. Wang, Y. Liu, X. Wu, D. Zhu, *Chem. Mater.*, **2003**, *15*, 1963-1969. [Crossref], [Google Scholar], [Publisher]

[12]. A. Rahimi, A. Schmidt, *Synlett*, **2010**, *9*, 1327-1330. [Crossref], [Google Scholar], [Publisher]

[13]. C.M. So, C.C. Yeung, C.P. Lau, F.Y. Kwong, *J. Org. Chem.*, **2008**, *73*, 7803-7806. [Crossref], [Google Scholar], [Publisher]

[14]. G.T. Baran, A. Menteş, *J. Organomet. Chem.*, **2016**, *803*, 30-38. [Crossref], [Google Scholar], [Publisher]

[15]. J. Xiao, Z. Lu, Y. Li, *Ind. Eng. Chem. Res.*, **2015**, *54*, 790-797. [Crossref], [Google Scholar], [Publisher]

[16]. A. Biffis, M. Zecca, M. Basato, *J. Mol. Catal. A Chem.*, **2001**, *173*, 249-274. [Crossref], [Google Scholar], [Publisher]

[17]. J. Horniakova, T. Raja, Y. Kubota, Y. Sugi, *J. Mol. Catal. A Chem.*, **2004**, *217*, 73-80. [Crossref], [Google Scholar], [Publisher]

[18]. K. Yu, W. Sommer, J.M. Richardson, M. Weck, C.W. Jones, *Adv. Synth. Catal.*, **2005**, *347*, 161-171. [Crossref], [Google Scholar], [Publisher]

[19]. C. Bolm, J. Legros, J. Paih, L. Zani, *Chem. Rev.*, **2004**, *104*, 6217-6254. [Crossref], [Google Scholar], [Publisher]

[20]. M.B. Gawande, P.S. Branco, R.S. Varma, *Chem. Soc. Rev.*, **2013**, *42*, 3371-3393. [Crossref], [Google Scholar], [Publisher]

[21]. C. Wang, X. Li, F. Wu, B. Wan, *Angew. Chem. Int. Ed.*, **2011**, *50*, 7162-7166. [Crossref], [Google Scholar], [Publisher]

[22]. M. Nasrollahzadeh, S.M. Sajadi, A. Rostami-Vartouni, M. Khalaj, *J. Mol. Catal. A Chem.*, **2015**, *396*, 31-39. [Crossref], [Google Scholar], [Publisher]

[23]. M. Nasrollahzadeh, S.M. Sajadi, A. Rostami-Vartooni, M. Bagherzadeh, R. Safari, *J. Mol. Catal. A Chem.*, **2015**, *400*, 22-30. [Crossref], [Google Scholar], [Publisher]

[24]. M. Nasrollahzadeh, S.M. Sajadi, A. Rostami-Vartooni, M. Bagherzadeh, *J. Colloid Interface Sci.*, **2015**, *448*, 106-113. [Crossref], [Google Scholar], [Publisher]

[25]. M. Nasrollahzadeh, S.M. Sajadi, A. Rostami-Vartooni, M. Khalaj, *J. Colloid Interface. Sci.*, **2015**, *453*, 237-243. [Crossref], [Google Scholar], [Publisher]

[26]. V. Tyler, The honest herbal, **1993**, 3rd edn, Pharmaceutical Products Press, New York. [Google Scholar], [Publisher]

[27]. D. Cloutier, A. Watson, *Weed Sci.*, **1985**, *33*, 358-365. [Crossref], [Google Scholar], [Publisher]

[28]. C. Kuo, L.J. Huang, H. Nakamura, *J. Med. Chem.*, **1984**, *27*, 539-544. [Crossref], [Google Scholar], [Publisher]

[29]. J.L. Wang, D. Liu, Z.J. Zheng, S. Shan, X. Han, S.M. Srinivasula, C.M. Croce, E.S. Alnemri, Z.

Huang, *Proc. Natl. Acad. Sci.,* **2000**, *97*, 7124-7129. [Crossref], [Google Scholar], [Publisher]

[30]. M.E. Zaki, H.A. Soliman, O.A. Hiekal, A.E. Rashad, *Naturforsch C*, **2006**, *61*, 1-5. [Crossref], [Google Scholar], [Publisher]

[31]. M.A. El Aleem, A.A. El Remaily, *Tetrahedron*, **2014**, *70*, 2971-2975. [Crossref], [Google Scholar], [Publisher]